JOURNAL OF MATERIALS SCIENCE **34** (1999) 439–444

Synthesis of $(Cr_XV_{1-X})_2O_3$ fine particles by a laser-induced vapor-phase reaction and their crystal structure

T. OYAMA, Y. IIMURA, K. TAKEUCHI
The Institute of Physical and Chemical Research (RIKEN), 2-1 Hirosawa, Wako-shi 351-01, Japan

T. ISHII
Department of Applied Chemistry, Science University of Tokyo, 1-3 Kagurazaka, Shinjuku-ku, Tokyo 162, Japan

Single-phase crystalline fine particles of $(Cr_xV_{1-x})_2O_3$ have been synthesized by a vapor-phase explosive reaction of a gas mixture of $CrO_2Cl_2 + VOCl_3 + H_2 + O_2$ induced by a single laser pulse. The distribution of particle size was uniform with a mean particle size of 80 nm. Lattice constants of $(Cr_xV_{1-x})_2O_3$ ($x = 0 - 1$) were accurately determined by the whole-powder-pattern decomposition (WPPD) method. A sharp increase in the *a* axis-length and a sharp decrease in the *c* axis-length of the hexagonal unit cell of the oxide ($x = 0.03$) have been observed. The crystal structures of $(Cr_xV_{1-x})_2O_3$ ($x = 0.15$, 0.5, 0.7) were studied by Rietveld analysis. © *1999 Kluwer Academic Publishers*

1. Introduction

Double oxides, which are solid solutions of metal oxides, are mainly synthesized by a liquid-phase or solid-phase reaction. Few examples have been reported for the syntheses of fine particles of a double oxide with a single phase by a vapor-phase reaction. Fine particles of $(Cr_xTi_{1-x})_2O_3$ have been synthesized in the present study by an explosive reaction ignited by dielectric gas breakdown induced by irradiating the reactant gas with an intensive laser pulse [1]. This method enjoys the following advantages: (1) the reaction is completed with one shot of a laser pulse, (2) fine particles of high purity can be obtained because contamination caused by the reaction with the material of the inner wall of the reactor hardly takes place; the temperature of the inner wall of the reactor does not become high, and (3) fine particles, whose metal composition is the same as that of the raw gas, with a narrow particle size distribution, can be obtained.

On the other hand, V_2O_3 is of special interest due to the fact that it has metallic conductivity at room temperature unlike other isostructural oxides Al_2O_3, Fe_2O_3, αGa_2O_3, Ti_2O_3, Cr_2O_3, In_2O_3, Tl_2O_3, and Rh_2O_3 despite its corundum structure. This is because it has a high hexagonal c/a ratio. It is also noteworthy that the addition of only 1% Cr^{3+} ion to V_2O_3 causes a sharp drop in c/a from 2.83 to 2.78 and the electric resistivity increases by several orders of magnitude [2, 3]. The refined crystal structures of 3.8% Cr-doped V_2O_3 solid solution has revealed that the structure distortion can be attributed to the fact that all the nearest neighbor V-V distances increase while the V-O distances remain unchanged [4].

In this study, fine particles of a Cr-V substitutional solid solution $(Cr_xV_{1-x})_2O_3$ ($x = 0 - 1$) were synthesized by our laser-induced vapor-phase reaction. Powder X-ray diffraction of the products was carried out, and the lattice constants were accurately determined using the WPPD method. The results of the crystal structure refinement by Rietveld analysis are also reported.

2. Experimental procedures

Gas mixtures of $CrO_2Cl_2 + VOCl_3 + H_2 + O_2$ with different mixing ratios were introduced into a 5*l* Pyrex reactor connected to a typical glass vacuum system through a greaseless stopcock. The vessel was baked out before the introduction. The pressure of the raw material gas was measured using an MKS Baratron capacitance manometer. A transversely excited atmospheric pressure (TEA) CO_2 laser (Lumonics 103) was used for the irradiation. The wavelength of a laser pulse, which is required to ignite gas breakdown, is independent of the raw materials; therefore, the P (26) line of the 10.6 μm branch at 939 cm^{-1}, one of the most intense radiation lines, was used to induce a dielectric gas breakdown and to ignite an explosive reaction. The reactant was irradiated with a laser pulse focused by a BaF_2 lens with a 200 mm focal length through a KBr optical window attached to the reactor. The pulse energy was 3.5–4.9 J, and the pulse duration was approximately 2 μs. The focused peak power density was therefore of the order of $GWcm^{-2}$. After the reaction, the reactor was evacuated overnight at 150 °C to remove any volatile and absorbed species. The produced powders were collected, and a powder specimen was

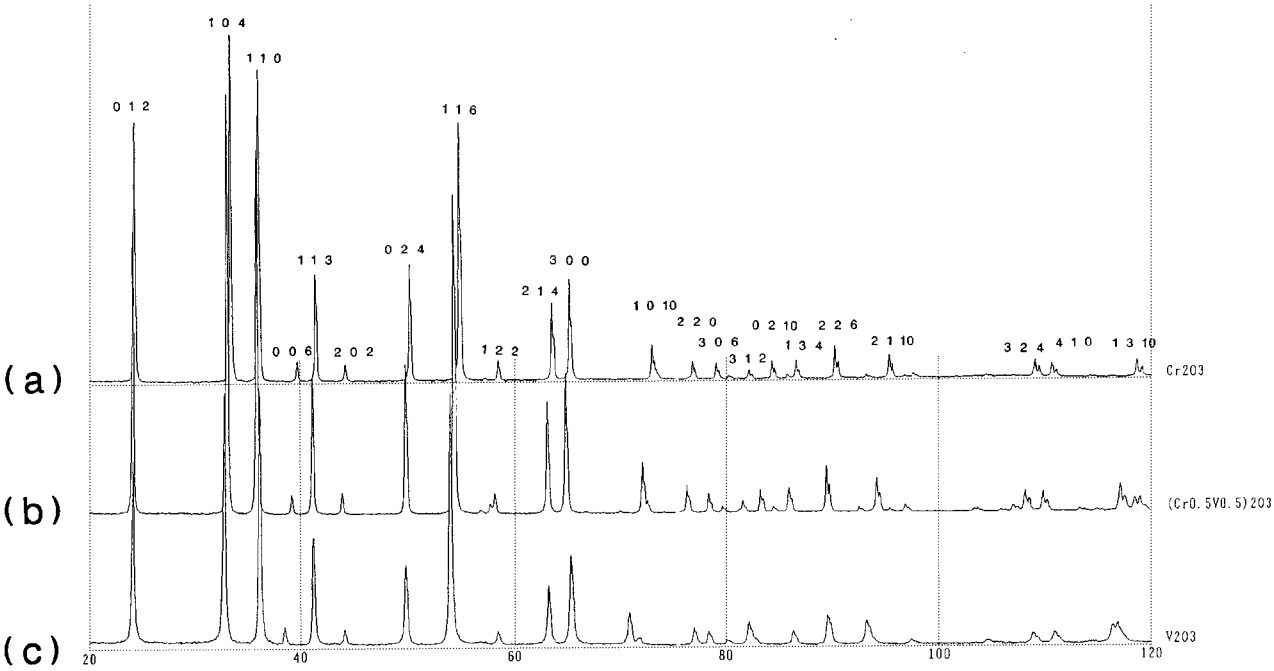

Figure 1 XRD patterns of the powders prepared from gas mixtures of (a) 1.33 kPa $CrO_2Cl_2 + 6.76$ kPa $H_2 + 1.33$ kPa O_2, (b) 1.07 kPa $CrO_2Cl_2 + 1.07$ kPa $VOCl_3 + 6.69$ kPa $H_2 + 1.35$ kPa O_2, and (c) 1.33 kPa $VOCl_3 + 6.67$ kPa $H_2 + 1.36$ kPa O_2.

packed on a glass specimen holder with a well depth of 0.2 mm. Diffraction data were collected on a Rigaku RAD-3R X-ray powder diffractometer. The experimental conditions were a Cu target X-ray tube, operated at 45 KV and 40 mA, 6° take-off angle, 1° divergent slit, 0.3 mm receiving slit, 0.6 mm receiving slit for a graphite monochromator (CuKα1, $\lambda = 1.5405981$ Å), and a scintilation counter with pulse height analyzer. The diffraction data were collected by step-scanning between 22.0° and 152° in 2θ with a step size of 0.02° and a counting time of 10 s per step for WPPD analysis and 2 s per step for Rietvelt analysis. NIST Si standard powder (SRM640b) was mixed with 20 weight % and was used as an internal standard for WPPD analysis. The sample temperature was maintained at 25 ± 0.2 °C throughout the experiment.

The particle size was measured from the particle images in the photograph taken by the transmission electron microscope (TEM, JEM-2000EX), and Cr/V contents in the particles were determined from the energy dispersive X-ray (EDX) spectra. Chromyl chloride and $VOCl_3$ were purchased from TRI Chemical Laboratory, Inc., and their purities were 99.9999% based on the metal analyses. Hydrogen and oxygen (Nippon Sanso, Inc., purity 99.9%) were used without further purification.

3. Results and discussion

3.1. Synthesis of $(Cr_xV_{1-x})_2O_3$ fine particles

When the raw gas was irradiated with one shot of a laser pulse, an explosion took place, accompanied by an orange luminescence. The resulting fine particles were deposited on the wall of the reactor. Fig. 1a–c shows the powder XRD patterns of the products produced in runs (a), (b), and (c), where gas mixtures of 1.33 kPa $CrO_2Cl_2 + 6.76$ kPa $H_2 + 1.33$ kPa O_2, 1.07 kPa $CrO_2Cl_2 + 1.07$ kPa $VOCl_3 + 6.69$ kPa $H_2 + 1.35$ kPa O_2, and 1.33 kPa $VOCl_3 + 6.67$ kPa $H_2 + 1.36$ kPa O_2 were used as the raw gas, respectively. The products of runs (a) and (c) were confirmed to be Cr_2O_3 and V_2O_3, respectively, because the determined values of the products of runs (a) and (c) were identical with those of Cr_2O_3 and V_2O_3 reported in the literature [5, 6]. Although peak shifts were observed in Fig. 1b, the product of the run (b) was speculated to be a single phase substitutional solid solution $(Cr_xV_{1-x})_2O_3$ of a corundum structure because the XRD pattern was identical with that of V_2O_3 and Cr_2O_3 reported in the literature. The powder XRD of the fine particles produced in the reactions of the gas mixtures, $CrO_2Cl_2 + VOCl_3 + H_2 + O_2$, was determined with different mixing ratios of the component. No diffraction line other than those of the corundum phase was observed in any of the products.

The EDX of these particles was measured. The results of the EDX analysis and a transmission electron micrograph of the product from a gas mixture of 1.07 kPa $CrO_2Cl_2 + 1.07$ kPa $VOCl_3 + 6.69$ kPa $H_2 + 1.35$ kPa O_2 are shown in Fig. 2. The Cu peak observed in the Fig. 2 is due to the sample holder. The atomic fractions of Cr ($x = \mathrm{Cr}/(\mathrm{Cr} + \mathrm{V})$), obtained from the peak heights of Cr and V at each measuring point (1, 2, 3, 4, 5, 6), were 0.50, 0.51, 0.52, 0.49, 0.48, and 0.51, respectively. These results indicate that the composition of V and Cr is the same in each particle; these values are the same as those of the raw gas mixtures. No Cl was detected in this analysis. It has been confirmed in the synthesis of a Cr-Ti double oxide that the results of EDX spectra, the composition of the raw gas, and the values determined by ICP emission spectrometry analysis were identical [1]. In Fig. 2, the TEM photograph of the produced fine particles, chains of primary particles, which are almost spherical and relatively uniform, are observed.

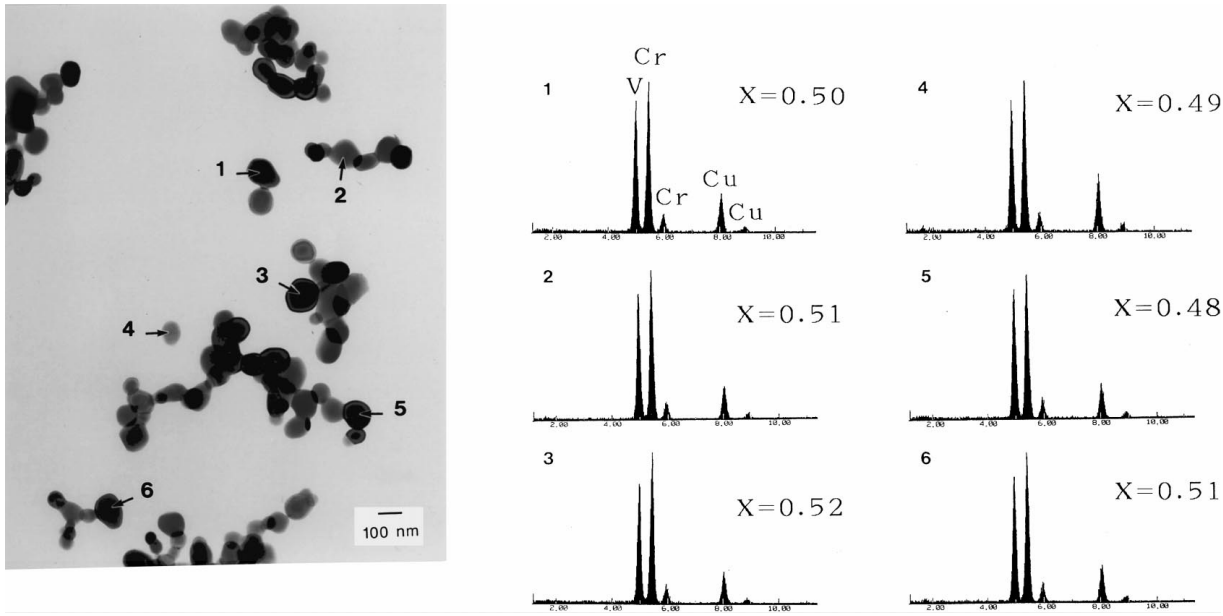

Figure 2 EDX spectra of as-produced particles from a gas mixture of 1.07 kPa CrO_2Cl_2 + 1.07 kPa $VOCl_3$ + 6.69 kPa H_2 + 1.35 kPa O_2.

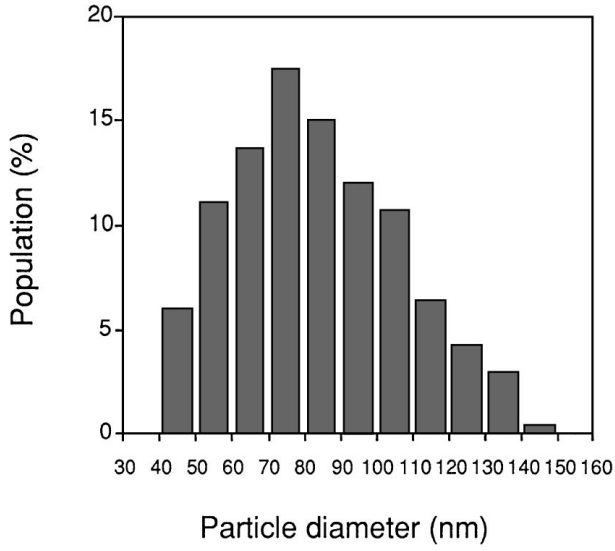

Figure 3 Particle-size distribution analysis of the products from a gas mixture of 1.07 kPa CrO_2Cl_2 + 1.07 kPa $VOCl_3$ + 6.69 kPa H_2 + 1.35 kPa O_2.

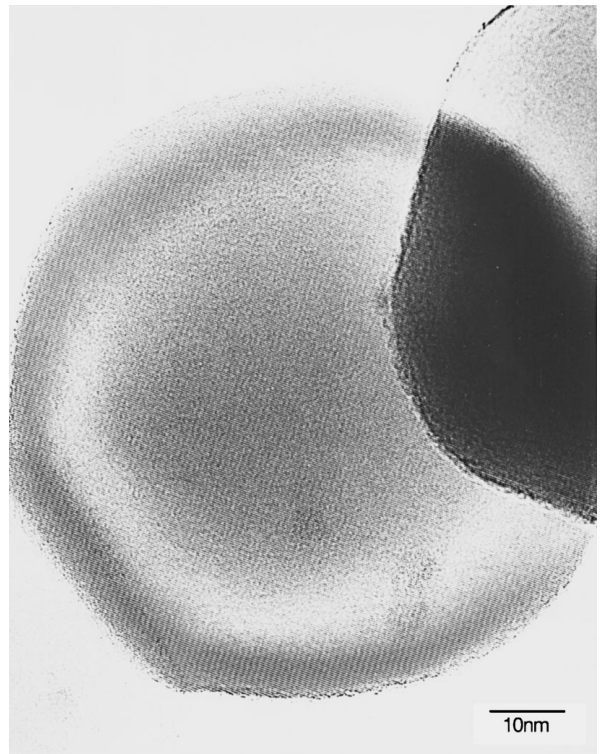

Figure 4 High-resolution transmission electron micrograph of as-produced particles from a gas mixture of 1.07 kPa CrO_2Cl_2 + 1.07 kPa $VOCl_3$ + 6.69 kPa H_2 + 1.35 kPa O_2.

Fig. 3 shows the particle size distribution obtained from the image of the TEM photograph. The high resolution TEM photograph of typical particles is shown in Fig. 4. The highly clear lattice image of (110) with a space of 2.7 Å, which is observed from the periphery to the center of a particle, indicates that the particles are highly crystalline. These observations show that they are spherical and crystalline ultrafine particles with a comparatively uniform particle size (mean particle size: 80 nm).

The lattice constants, a and c, of $(Cr_xV_{1-x})_2O_3$ $(x = 0 - 1)$ have been determined accurately by the WPPD method using the program WPPF (version 1.2) [7]. Further, the relationship between lattice constant ratios c/a and unit cell volumes, and the atomic fractions, x of Cr, was examined. Table I and Figs 5, 6, and 7 show the results. The reliability factor R_p, R_{wp}, and R_{pe} are defined as follows:

$$R_p = \Sigma|y_i(o) - y_i(c)|/\Sigma|y_i(o)| \quad (1)$$

$$R_{wp} = \{\Sigma w_i[y_i(o) - y_i(c)]^2/\Sigma w_i[y_i(o)]^2\}^{1/2} \quad (2)$$

$$R_{pe} = \Sigma|y_i(o) - y_i(c)|/\Sigma|y_i(o) - b_i(c)| \quad (3)$$

Here, $y_i(o)$ and $y_i(c)$ are the observed and calculated intensities at i, w_i is the ith weight, and

TABLE I *R* factor and lattice constants of $(Cr_xV_{1-x})_2O_3$ determined by WPPD method

x	R_p/%	R_{wp}/%	R_{pe}/%	a/Å	c/Å	c/a	V/Å^3
0.00	8.34	11.02	12.3	4.95086(6)	14.0029(3)	2.8284	297.2
0.00[a]				4.9540(2)	14.0083(10)	2.8277	297.7
0.01	5.76	8.66	7.82	4.95382(4)	13.9927(4)	2.8246	297.4
0.03	5.40	8.01	7.17	4.99682(2)	13.9318(2)	2.7881	301.2
0.11	5.86	8.68	7.80	4.99564(4)	13.8937(4)	2.7812	300.3
0.15	5.27	8.02	6.95	4.99532(3)	13.8748(2)	2.7776	299.8
0.22	5.25	7.98	7.05	4.99346(3)	13.8489(1)	2.7736	299.1
0.30	5.88	8.83	7.80	4.99039(4)	13.8231(1)	2.7699	298.1
0.40	5.58	8.24	7.22	4.98654(3)	13.7842(1)	2.7643	296.8
0.50	4.98	7.59	6.34	4.98340(3)	13.7555(1)	2.7603	295.8
0.60	4.89	7.51	6.13	4.97859(2)	13.72000(9)	2.7558	294.5
0.65	4.76	7.42	5.95	4.97672(2)	13.70494(3)	2.7474	294.0
0.75	5.35	8.53	6.68	4.97175(3)	13.6730(1)	2.7501	292.7
0.90	5.60	8.31	8.91	4.96373(3)	13.6201(1)	2.7439	290.6
1.00	5.16	7.83	7.49	4.95845(3)	13.5948(1)	2.7417	289.5
1.00[b]	6.06	8.59	7.22	4.95922(2)	13.59690(7)	2.7417	289.6
1.00[c]				4.95916(12)	13.5972(6)	2.7418	289.6
1.00[d]				4.95876(14)	13.5942(7)	2.7415	289.5

[a]Reference 6.
[b]Cr_2O_3(SRM674), this analysis.
[c]Cr_2O_3(SRM674), NIST certified value.
[d]Reference 5.

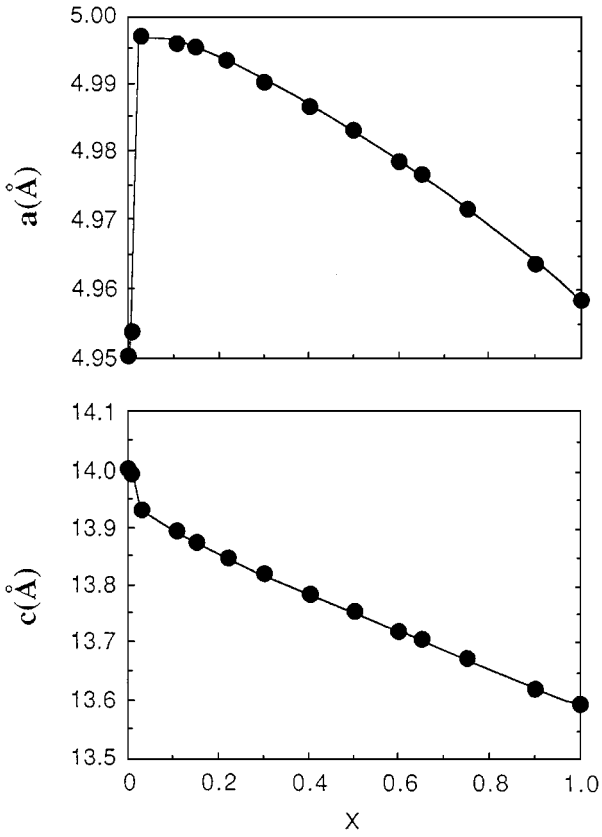

Figure 5 Lattice constants *a* and *c* as a function of *x* in $(Cr_xV_{1-x})_2O_3$.

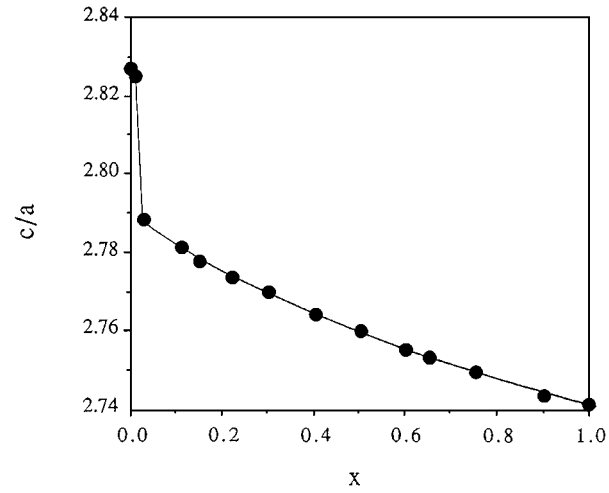

Figure 6 Lattice constant ratios c/a as a function of *x* in $(Cr_xV_{1-x})_2O_3$.

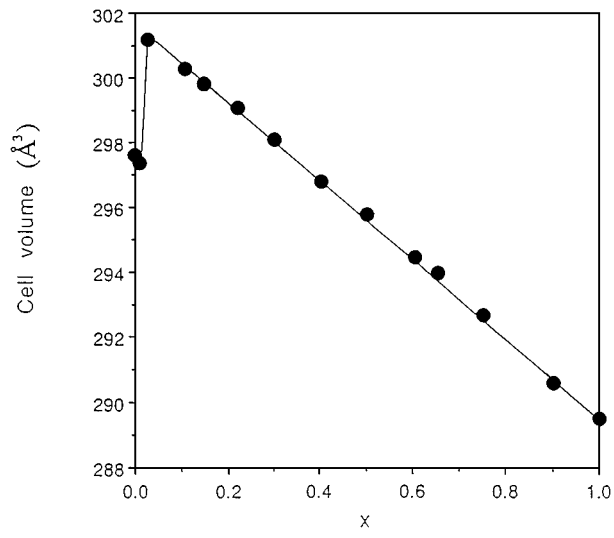

Figure 7 Unit cell volumes as a function of *x* in $(Cr_xV_{1-x})_2O_3$.

$b_i(c)$ is the calculated background intensity. The lattice constants ($a = 4.95922(2)$, $c = 13.59690(7)$) of Cr_2O_3(SRM674) determined by WPPD method agree with the NIST certified values ($a = 4.95916(12)$, $c = 13.5972(6)$) within the standard deviation. The lattice constants ($a = 4.95845(3)$, $c = 13.5948(1)$) of Cr_2O_3 (produced by this experiment) determined by WPPD method agree with the reported values

($a = 4.95876(14)$, $c = 13.5942(7)$) within 2σ [5]. As is seen in the figures, the lattice constant a dramatically expanded from 4.95086 to 4.99682 Å, while lattice constant c decreased from 14.0029 to 13.9318 Å. The substitution of V in the V_2O_3 for Cr by 3% increased the lattice constant a by 0.93%. The lattice constant a decreased gradually with increasing atomic fraction of Cr ($x = 0.03$–1.0). On the contrary, the lattice constant c decreased by 0.51% on substituting V for Cr by 3%, and when x was larger than 0.1, it decreased linearly. The ratio of c/a decreased by 1.4% when V_2O_3 was substituted for Cr ($x = 0.03$) and decreased with increasing x. The unit cell volume showed a maximum, 301.2 Å^3 at $x = 0.03$, and it decreased linearly with increasing x. The behavior of the unit-cell volumes are similar to that of the a-axis in these systems. The colors of V_2O_3 and Cr_2O_3 were black and light green, respectively, while that of the Cr-V double oxide became more and more greenish with the increasing x of Cr.

3.2. Crystal structure

It is suggested from the XRD powder pattern that $(Cr_xV_{1-x})_2O_3$ is a solid solution with the substitution of Cr by V at the position of the crystal structure of Cr_2O_3. The structure refinement was carried out by employing the Rietveld method using the computer program RIETAN (Version RINT) [8]. The diffraction intensity data profiles collected from the range 22.0–112.0° were used because of the limitation of the program. The refinement was started using the R$\bar{3}$C space group and the structure parameters of Cr_2O_3 were derived from Newnham and de Haan [9]. The composition of Cr and V has been determined by EDX measurement. Common isotropic thermal parameters were assigned to the Cr(V) metals. It was assumed that there is no preferred orientation of the crystallites with isotropic fine particles. The lattice constants have been obtained from the WPPD method and used for the Rietveld method. The reliability factors are the same as in Equations 1 and 2, respectively. Re, R_B, and S are defined as follows:

$$R_e = \{(N_p - N_r - N_c)/\Sigma W_i[y_i(o)]^2\}^{1/2} \quad (4)$$

$$R_B = \Sigma|I_K(\text{`}o\text{'}) - I_K(c)|/\Sigma I_K(\text{`}o\text{'}) \quad (5)$$

$$S = R_{wp}/R_{pe} \quad (6)$$

Here, Np is the number of intensity data, Nr is the number of refined parameters, Nc is the number of constrained parameters, and I_K is the intensity assigned to the Kth Bragg reflection at the end of the refinement cycles. Calculated reliability factors for $(Cr_{0.5}V_{0.5})_2O_3$ were $R_P = 9.74\%$, $R_{WP} = 12.77\%$, $R_e = 5.28\%$, $R_B = 2.14\%$, $S = 1.21$, all of which showed high reliability. Fig. 8 illustrates the profile fit and the difference patterns for the oxide. A fair coincidence is seen between the observed values and calculated ones in Fig. 8. These results prove that the Cr-V oxide is a solid solution of a substitution type. The refined structure parameters are listed in Table II. The atomic coordinates of $Z(R)$ are identical with that of $Cr_2O_3 \pm 3\sigma$ but differ somewhat from that of V_2O_3. The atomic coordinate of X(O) is identical with that of Cr_2O_3 and V_2O_3. It has been observed that V_2O_3 is unique among corundum oxides with respect to the $R_1 - R_3$ distance across the shared octahedral edge. This metal-metal distance was shown to be anomalously short for V_2O_3 by the plot of $R_1 - R_3$ versus the effective ionic radii of R [10]. As is shown in Table II, the distance of $R_1 - R_2$, whose ionic radii are very short, increased by *ca* 1.4% from 2.701 Å ($x = 0$) to 2.7379 Å ($x = 0.15$), and the distance of $R_1 - R_3$

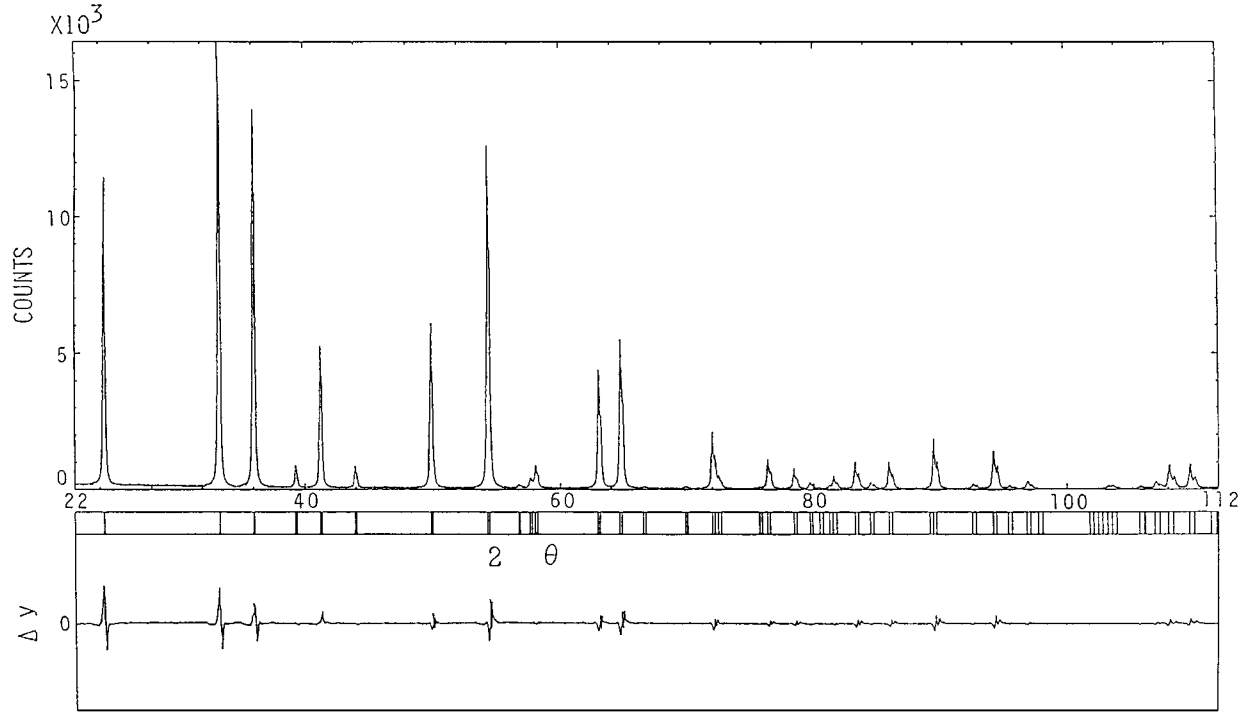

Figure 8 X-ray Rietveld refinement of $(Cr_{0.5}V_{0.5})_2O_3$. The solid line is the best-fit profile, and the points superimposed on it are the raw data. The differences between the observed and calculated intensities, $\Delta y = y_i(o) - y_i(c)$, are shown by points appearing at the bottom. Tick marks below the profile indicate the positions of all allowed Kα1 and Kα2 peaks.

TABLE II Crystal data for Cr_2O_3, $(Cr_{0.70}V_{0.30})_2O_3$, $(Cr_{0.5}V_{0.5})_2O_3$, $(Cr_{0.15}V_{0.85})_2O_3$, V_2O_3 (Notation after Newnham and de Haan[a])

	Cr_2O_3[a]	$(Cr_{0.70}V_{0.30})_2O_3$	$(Cr_{0.50}V_{0.50})_2O_3$	$(Cr_{0.15}V_{0.85})_2O_3$	V_2O_3[a]
a_H (Å)	4.9607(10)	4.97342(5)	4.98340(3)	4.99532(3)	4.952(1)
c_H (Å)	13.599(5)	13.6895(2)	13.7555(1)	13.8748(2)	14.002(5)
z (R)	0.3475(3)	0.3479(2)	0.3483(3)	0.3487(3)	0.3463(3)
x (O)	0.306(4)	0.307(2)	0.306(2)	0.307(2)	0.315(4)
Rp (%)		7.95	9.74	9.25	
R_{wp} (%)		10.48	12.77	12.48	
Re (%)		7.02	10.59	10.71	
R_B (%)		1.87	2.14	2.62	
S		1.49	1.21	1.17	
			Interatomic distances in (Å)		
R1-O1(3)	2.02(2)	2.0301(4)	2.0397(6)	2.05551(7)	2.06(2)
R1-O5(3)	1.97(1)	1.9678(2)	1.9708(4)	1.9749(5)	1.96(1)
R1-R2(1)	2.65(1)	2.6815(4)	2.7055(5)	2.7379(7)	2.70(1)
R1-R3(3)	2.89(0)	2.8991(1)	2.9066(1)	2.9152(1)	2.88(0)
R1-R4(3)	3.43(0)	3.4329(2)	3.4366(3)	3.4464(4)	3.47(0)
R1-R5(6)	3.65(4)	3.6566(2)	3.6672(3)	3.6893(4)	3.69(0)
O1-O2(2)	2.63(4)	2.6403(9)	2.644(1)	2.655(2)	2.70(4)
O1-O3(4)	2.99(2)	2.9936(5)	3.0001(7)	3.0051(9)	2.94(2)
O1-O4(2)	2.74(1)	2.7536(2)	2.7642(3)	2.7837(4)	2.81(1)
O1-O5(4)	2.85(1)	2.8623(2)	2.8734(3)	2.8909(3)	2.89(1)

[a]Reference 9.

increased by *ca* 1.2% from 2.880 Å ($x = 0$) to 2.9152 Å ($x = 0.15$). Nevertheless, V^{3+} was substituted for Cr^{3+}, whose radius is 17% smaller than that of V^{3+}. These distances, however, decreased when the Cr fraction was increased further. Regarding the distances between O atoms, the distance of $O_1 - O_3$ increased by 2.2% when the fraction of Cr was 0.15 ($x = 0.15$), and decreased when the fraction of Cr was increased further. This increase in the metal-metal distance is consistent with the observations by Dernier [4].

4. Conclusions

It is concluded that (1) fine particles of the Cr-V double oxide were synthesized by an explosive chain reaction of a gas mixture of $CrO_2Cl_2 + VOCl_3 + H_2 + O_2$ induced by a single-pulse irradiation from a TEA-CO_2 laser, (2) the products were single-phase, uniform, and crystalline fine particles of a spherical form (mean radius: 80 nm), (3) the product was a substitutional solid solution $(Cr_xV_{1-x})_2O_3$, which was indicated by the XRD result, (4) a sharp increase in the *a*-axis length and a decrease in the *c*-axis length of the hexagonal unit cell of the double oxide were observed in the accurate determination of the lattice constants of the $(Cr_xV_{1-x})_2O_3$ ($x = 0 - 1$) using the WPPD method, and (5) the nearest neighbor V-V distances in the Cr-doped crystals were longer, compared with those in V_2O_3, which was shown by the Rietveld analysis of the crystal structure of the $(Cr_xV_{1-x})_2O_3$ ($x = 0.15$, 0.5).

References

1. T. OYAMA, Y. IIMURA, T. ISHII and K. TAKEUCHI, *J. Mater. Sci. Lett.* **11** (1992) 1573.
2. R. E. NEWNHAM and Y. M. DE HAAN, Progress Rep. No. XXXVI. Lab. Insulation Research, p. 11. Massachusetts Institute of Technology (1960).
3. A. J. MCMILLAN, Tech. Rep. No. 172. Lab. Insulation Research, Massachusetts Institute of Technology (1962).
4. P. D. DERNIER, *J. Phys. Chem. Solids.* **31** (1970) 2569.
5. H. F. MCMURDIE, M. C. MORRIS, E. H. EVANS, B. PARETZKIN, W. WONG-NG, Y. ZHANG and C. R. HUBBARD, *Powder Diffraction* **2** (1987) 45.
6. PDF 34–187.
7. H. TORAYA, *J. Appl. Cryst.* **19** (1986) 440.
8. F. IZUMI, *Nippon Kessyo Gakkaishi* (*J. Crystallogr. Soc. Jpn*) **27** (1985) 23.
9. R. E. NEWNHAM and Y. M. DE HAAN, *Z. Krist.* **117** (1962) 235.
10. C. T. PREWITT and R. D. SHANNON, *Trans. Am. Crystallogr. Ass.* **5** (1969) 56.

Received 12 August
and accepted 26 August 1998